

## Deep Electrical Structure of Taiwan as Inferred From Magnetotelluric Observations

Chow-Son Chen<sup>1</sup>, Chien-Chih Chen<sup>1</sup> and Keyson Chou<sup>1</sup>

(Manuscript received 3 May 1997, in final form 14 January 1998)

### ABSTRACT

Not until magnetotellurics (MT) were conducted, was very much known about the deep electrical structures beneath Taiwan. Finally, the first MT was used as part of an integrated project to map 3-D structures; subsequently, nineteen MT soundings, uniformly covering the entire Taiwan area, were conducted and analyzed to map 3-D resistivity distributions.

Results show the existence of a distinct low resistivity zone (less than 160 ohm-m) in the uppercrust with depths ranging about 10-20 km and about 30° northward dipping near the latitude of 24.5°N beneath Taiwan. This finding is undoubtedly the most significant feature obtained by means other than from seismicity, which provides evidence of the Philippine Sea plate subduction northward beneath Taiwan. Based on the temperature estimates from the MT results, it is inferred that the main cause of this low resistivity zone is most probably the fluids released from dehydration reactions. The Moho discontinuity defined by velocity contrast at depth about 40-50 km does not seem to correspond with any sharp boundary which could be traced in the resistivity profiles.

( Key words: MT, Electrical structures, Dehydration, Taiwan, Subduction )

### 1. INTRODUCTION

Knowledge of the deep structure of Taiwan has substantially increased over the past decade with the powerful tool of seismic imaging and the accumulation of geologic information (Wu, 1978; Aki, 1982; Tsai, 1986; Roecker *et al.*, 1987; Thurber and Aki, 1987; Wang, 1988; Rau and Wu, 1995; Ma *et al.*, 1996). However, the very causes of the observed deep crustal reflection, such as the composition and nature of the crust, are basically unknown. Accordingly, it is generally recognized that not mere seismic reflection but other geophysical information as well needs to be included in the interpretation. The purpose of this paper is to study the deep resistivity structure and the associated tectonic problems by using the newly established deep sounding tool - magnetotellurics (MT).

A considerable number of experimental MT studies have been reported since the MT theory was first proposed (Cagniard, 1953). It is well documented that MT can help to solve

---

<sup>1</sup>Institute of Geophysics, National Central University, Chung-Li, Taiwan, ROC

the diversity of intensely convoluted and intruding tectonic and geothermal problems. Valuable case histories include those on tectonically disturbed regions ( Vozoff, 1972; Ward, *et al.*, 1971; Young and Kitchen, 1989 ) and geothermal areas (Stanley *et al.*, 1977). After studying six examples in which the MT results aided the geological/tectonic interpretations of the seismic sections, Jones (1987) proposed that a collocated MT study should, in almost every case, be conducted wherever a seismic reflection survey is undertaken because the electrical structure would provide powerful constraints on the interpretation of the deep reflection horizon.

This first MT survey in the Taiwan region was operated by the Institute of Geophysics, National Central University. The MT results in this study not only show a satisfactory correlation between the surface geology and deep tectonic map, but also provide one of the geophysical constraints, other than seismicity, of Taiwan orogeny.

## 2. MT ACQUISITION AND PROCESSING

A tensor MT survey was carried out to map the deep resistivity structure of Taiwan. A Phoenix V5-MT system, manufactured in Canada by Phoenix Geophysics, was used. It processes data in real time, covering a frequency range of 384 to 0.00055 Hz. Measurements were made using five field components including two electric fields ( $E_x$  and  $E_y$ ) and three magnetic fields ( $H_x$ ,  $H_y$  and  $H_z$ ) in acquiring an MT sounding (Figure 2). A remote reference (Gamble, *et al.*, 1979) using two additional components  $H_x$  and  $H_y$  was sometimes used, depending on the site spacing, so as to suppress electromagnetic noise present at the site. Although 37 MT soundings have been made at locations uniformly covering the entire Island of Taiwan since December 1995, this study confined its analysis to those data of better quality, i.e. those of the 19 sites shown in Figure 1.

The longer period data were mostly collected over a time span from about 12 up to 18 hours, while the shorter period data were 4 hours. The time series of the electric and magnetic field variations were first converted into the frequency domain by the Fourier transformation. The Fourier coefficients for a given frequency were then assumed to be related through the tensor equation ( Vozoff, 1972):

$$\begin{bmatrix} E_x \\ E_y \end{bmatrix} = \begin{bmatrix} Z_{xx} & Z_{xy} \\ Z_{yx} & Z_{yy} \end{bmatrix} \begin{bmatrix} H_x \\ H_y \end{bmatrix}, \quad (1)$$

where  $E_x$  and  $E_y$  are electric fields along the N-S and E-W directions, respectively;  $H_x$  and  $H_y$  are the corresponding magnetic fields, and  $Z_{xx}$ ,  $Z_{yx}$ ,  $Z_{xy}$  and  $Z_{yy}$  are the elements of the impedance tensor  $Z$  which includes information as to the electric conductivity distribution of earth. The robust process (Jones *et al.*, 1989) was then used to reduce the variances of the off-diagonal MT impedance.

In a strictly 1-D situation, the diagonal terms ( i.e.  $Z_{xx}$  and  $Z_{yy}$  ) of the impedance tensor  $Z$  become zero, which allows for the computation of the apparent resistivity and phase from the data. However, if the underlying structure is 2-D, then the impedance tensor can be rotated such that the diagonal terms are minimized in the sense of the least-square error. The direction

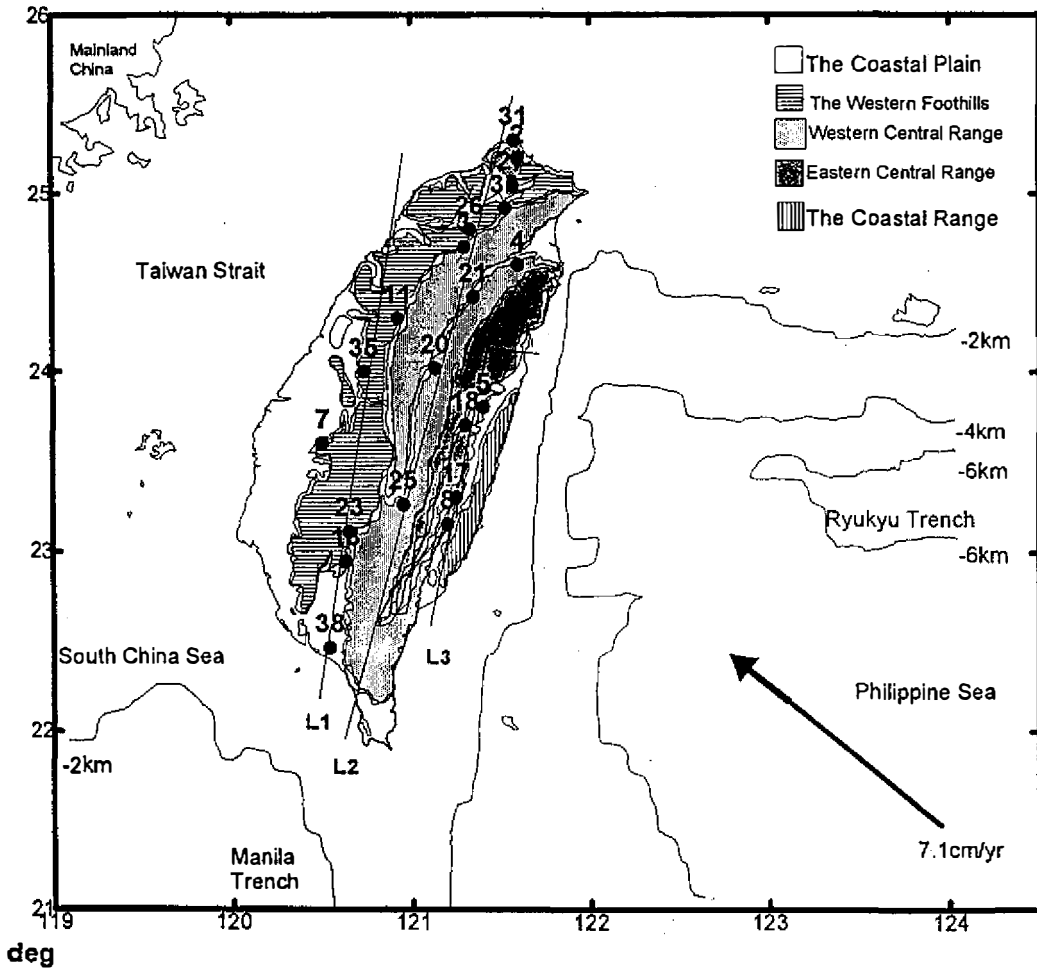
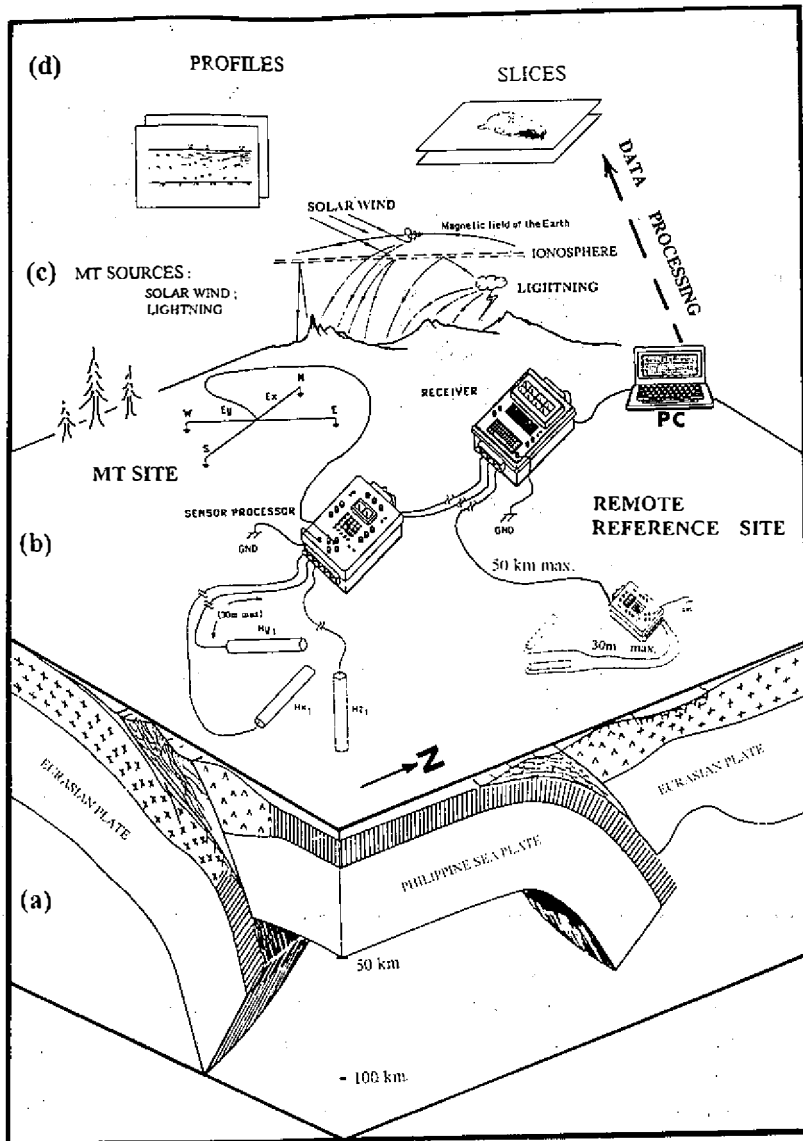


Fig. 1. Tectonic setting and bathymetry of Taiwan and the surrounding area (Suppe, 1981). The vector of relative motion between the Philippine Sea plate and the Eurasian plate is shown by the arrow. The main geological divisions of Taiwan are also indicated. The locations of the MT soundings are indicated by solid circles. Interpretation profiles are indicated by L1, L2 and L3.

determined from this procedure is known as the regional electrical strike direction. According to Swift (1967), the regional strike direction ( $\theta$ ) is obtained from:

$$\tan 4\theta = \frac{2\text{Re}[(Z_{xy} + Z_{yx})(Z_{xx} - Z_{yy})]}{[|Z_{xx} - Z_{yy}|^2 - |Z_{xy} + Z_{yx}|^2]} \quad (2)$$



*Fig. 2.* Magnetotelluric (MT) field layout in Taiwan. (a) Plate tectonic setting beneath Taiwan (Ho, 1975). (b) MT field layout: V5-MT (Phoenix Geophysics, Canada), a real-time processing system, with the capability to measure the frequency band range of 384 to 0.00055 Hz. The measurements were made by using five field components and a remote reference. (c) MT sources mainly coming from solar wind and lightning. (d) On-site data processed by a PC showing horizontal depth slices and vertical profiles. These geoelectric maps illustrate the 3D conductivity structures of Taiwan.

where \* indicates the complex conjugate. The average values of the regional strike of the impedance tensor  $Z$  over the entire frequency range for each site, with few exceptions, is about N-S. Here, an N-S regional trend of  $Z$  was adopted for all sites as well as frequencies, and all data were rotated in that direction for use in subsequent analyses.

The rotated data could then be converted into their apparent resistivity and phase plots as a function of frequency by (Cagniard, 1953):

$$\rho_{ij} = \frac{|Z_{ij}|^2}{\omega\mu} \quad \text{and} \quad (3)$$

$$\phi_{ij} = \tan^{-1} \left[ \frac{\text{Im } Z_{ij}(\omega)}{\text{Re } Z_{ij}(\omega)} \right], \quad (4)$$

where  $\rho_{ij}$  is the resistivity;  $\omega$  and  $\mu$  are angular frequency and magnetic permeability, respectively;  $\text{Re}(Z_{ij})$  and  $\text{Im}(Z_{ij})$  are the real and imaginary parts of tensor elements  $Z_{xy}$  or  $Z_{yx}$ .

In the 2-D case,  $\rho_{xy}$  and  $\phi_{xy}$  are referred to as the TE mode (or E-polarization, which is actually or parallel to the strike), and  $\rho_{yx}$  and  $\phi_{yx}$  the TM mode (or B-polarization). Figures 3a and 3b show the apparent resistivity and the phase angle for each site, respectively. It is worth noting that the phase angle plot can greatly assist in the assessment of the MT data quality of each sounding; the smoothed phase data suggest that the experimental signal to noise ratio is quite satisfactory since phase is relatively sensitive to noise disturbances.

The use of invariant impedance (Ingham, 1988) may minimize any possible erroneous interpretation of MT data which can occur when the 1D modeling of the TE mode is carried out. Furthermore, the possibility of erroneous interpretation occurs in the vicinity of near-surface 3-D conductivity anomalies. Therefore, the apparent resistivities and phases used in the 1D modeling are those calculated from the invariant impedance:

$$Z_{\text{inva}} = (Z_{xy} Z_{yx})^{0.5} \quad \text{and} \quad (5)$$

$$\phi_{\text{inva}} = 0.5 (\phi_{xy} + |\pi + \phi_{yx}|). \quad (6)$$

Then the Occam's inversion (Constable et al. 1987), which produces a model that is maximally smooth in resistivity structure, was used to produce the 1D model at each sounding data. The reasons for employing Occam's inversion are: (1) the results of the Occam's inversion are very similar to a highly smoothed resistivity log and therefore easily understood, especially in the reconnaissance stage, and (2) there is no need to preset an initial model for Occam's inversion, and the inversion results are unique. Some of those results are shown in Figure 4. The horizontal scale is  $\log_{10}$  (resistivity) in ohm-m, while the vertical scale is  $\log_{10}$  (depth) in meters. The location of each site is shown in Figure 1. Note the important feature of

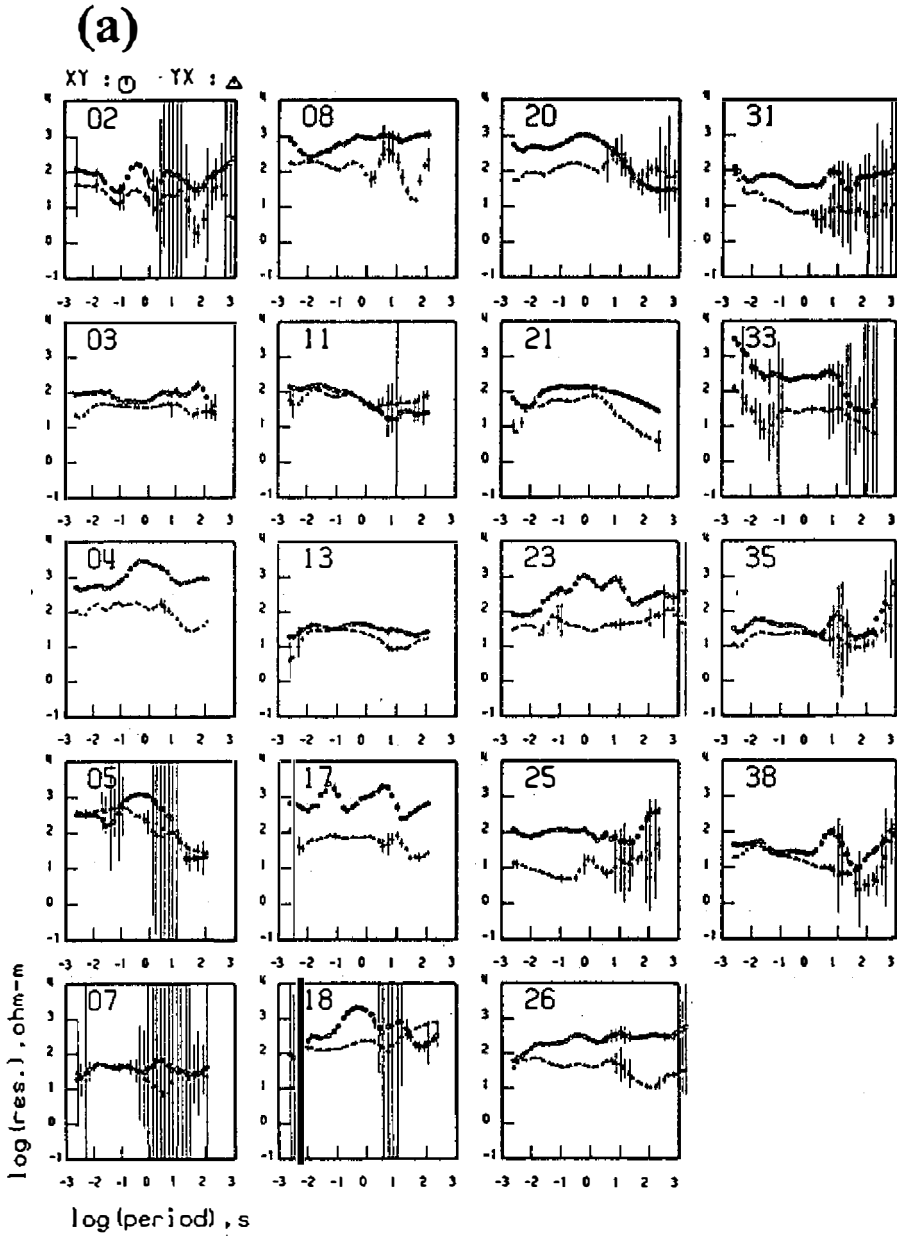
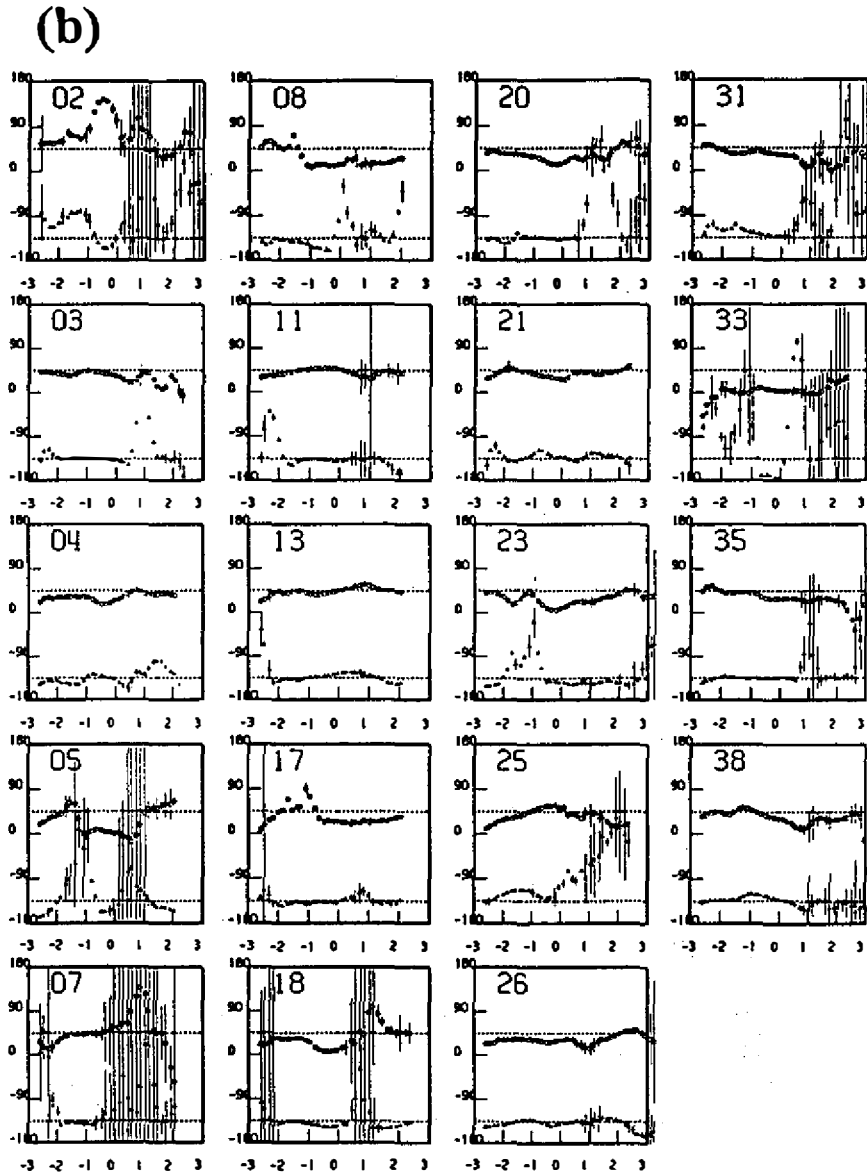


Fig. 3. (a) Apparent resistivities and (b) phases in the Taiwan area. The horizontal scale is  $\log_{10}$  (period) in seconds. The vertical scale for the apparent resistivity is  $\log_{10}$  (resistivity) in ohm-m; that for phase is in degrees. The TE and TM mode are indicated by circles and triangles, respectively. The location of each site is shown in Fig. 1. Two dotted lines, indicating  $45^\circ$  and  $-135^\circ$ , are superimposed on each phase plot to show half-space response.



(Continued)

the existence of a conductive zone (arrows in Figure 4) at depths around 10-20 km beneath each sounding. The geologic significant is the main topic of discussion in this paper.

In order to assess the subsurface 3-D resistivity structures of Taiwan quantitatively, horizontal depth slices at different depths and vertical N-S profiles were constructed. Before those slice maps and profiles were constructed, the trend surface analysis technique (Davis, 1973) was employed for the sake of greater clarity. Figure 5 shows the results of a 1-km slice map

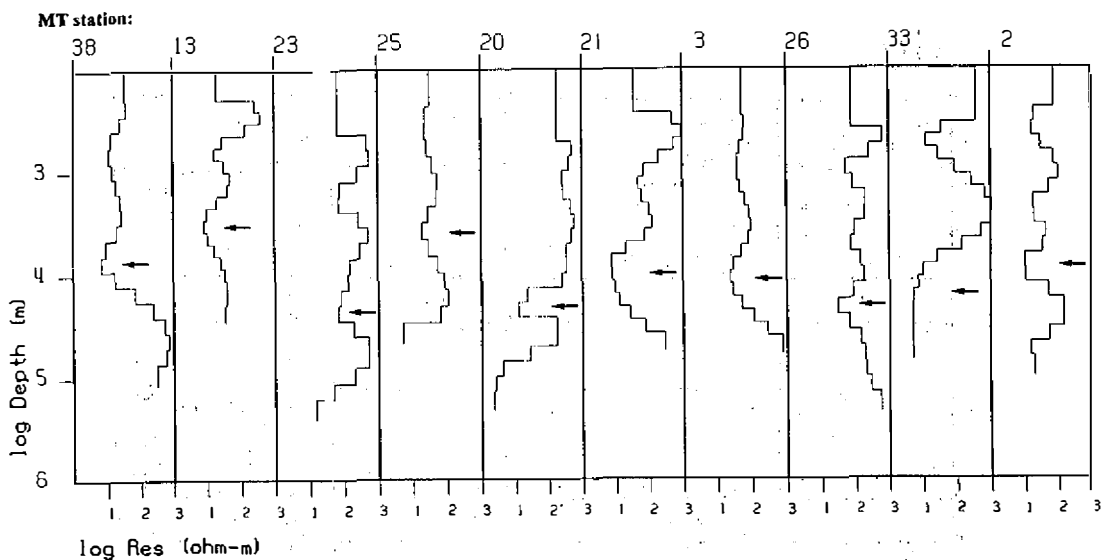


Fig. 4. Some Occam's inversions showing resistivities versus depth in the Taiwan area. The horizontal scale is  $\log_{10}$  (resistivity) in ohm-m, while the vertical scale  $\log_{10}$  (depth) is in meters. The location of each site is shown in Fig. 1. Note the important feature of the presence of a conductive zone (arrow) at depths around 10-20 km beneath each sounding.

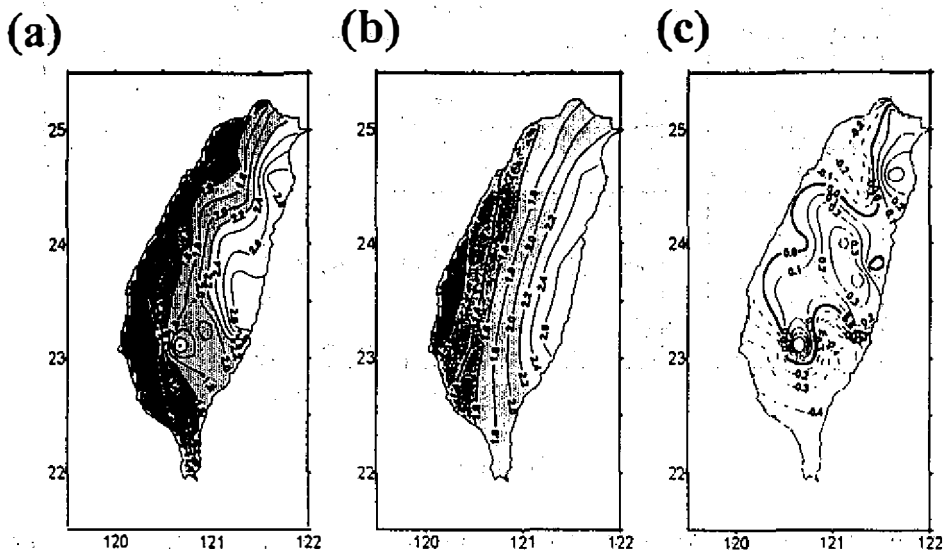


Fig. 5 (a) Resistivity contour map at the depth of 1 km in the Taiwan area. (b) Second-degree trend surface. (c) Contoured residuals from the second-degree trend surface. The regional trend shows resistivities of the NNE trend which are hardly discernible on the observed resistivity map in (a).

after being processed by trend surface analysis techniques. The regional diagram (Figure 5b) when compared to the diagram before the trend surface analysis (Figure 5a) reveals clear trends for the identification of the resistivity patterns. The refinement of the images of the MT data by proper filtering is of significance especially for the complicated structures frequently met around the plate boundary, such as those in Taiwan.

### 3. RESULTS

#### 3.1 Horizontal Depth Slices

Figure 6 shows the resistivity depth slices at depths 5, 10, 15, 20, 30 and 40 km. The value of the contours is  $\log_{10}$  (resistivity) in ohm-m units. At shallow depths of less than 5 km, the resistivity trend demonstrates a NNE-SSW strike which is oriented in approximately the same direction as the main geological provinces of Taiwan (Figure 1). The resistivities in this depth slice decrease to the west and are closely correlated to the variations in the surface geology of Taiwan, from the metamorphic basement of the Central Range to the thick sediments of the Coastal Plain. The iso-resistivity line  $10^{1.8}$  ohm-m separates the Western foothills to the west and the Central Range to the east, while the iso-resistivity lines  $10^{3.0}$  ohm-m divide the Central

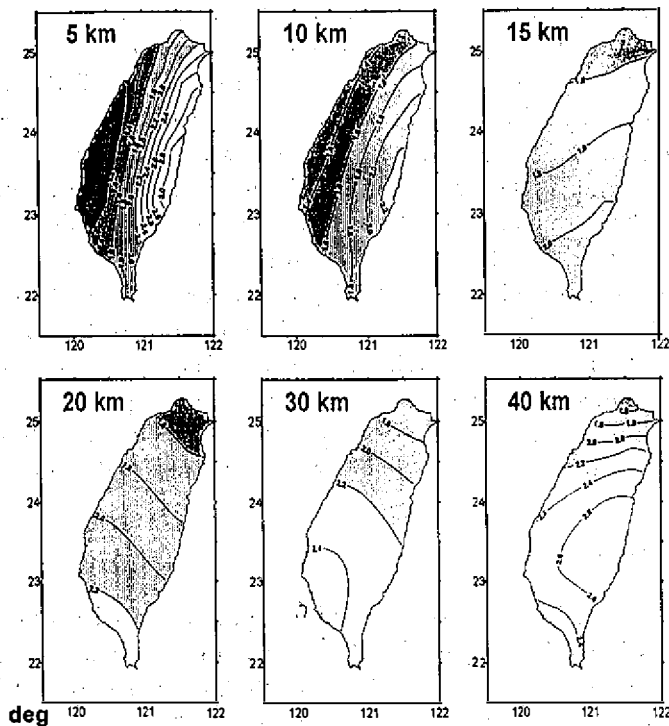


Fig. 6. Resistivity, in  $\log_{10}$  (resistivity) ohm-m, contour maps at depths 5, 10, 15, 20, 30 and 40 km, respectively. The shaded area indicates the low resistivity anomaly, less than  $10^{2.2}=150$  ohm-m.

Range to the west and the Longitudinal Valley to the east.

As depth increases to 10 km, the whole island demonstrates two main areas with the iso-resistivity line  $10^{1.6}$  ohm-m separating the low resistivity zone to the west and the high resistivity one to the east. Meanwhile, in comparison with the resistivity pattern at shallow depths (less than 5 km), the gradient of the contour lines becomes smaller suggesting a decrease in the resistivity contrast between eastern and western Taiwan; in other words, the electrical response of the main geologic zonations of Taiwan diminish at this depth.

As depth further increases to more than 15 km, the resistivity trend changes abruptly to a NE-SW and then to a NW-SE strike with resistivity values decreasing to the north. The existence of the low resistivity center in the northern part of Taiwan is probably related to the Tatun geothermal area. Wang (1988) studied the b-value distribution of shallow earthquakes (less than 35 km) in Taiwan and recognized a zone with a large b-value in the northern part of the region which is probably related to the remnant geothermal effect after past volcanic activities. Ma *et al.* (1996) also observed the low P-wave velocity in the northern part of Taiwan at depths less than 10 km (actually extending to 20 km in their plots). The MT results in the present study with a low resistivity zone in the north are not only in good agreement with theirs, but also provide a clear vivid description by means of 3-D images. Hence, the low resistivity which extends to depths greater than 40 km in the northernmost part of Taiwan must be due to the remnant geothermal effect after past volcanic activities.

Additionally, in the depth range of 15-20 km, the low resistivity anomaly (less than  $10^{2.2}$  ohm-m) covers the entire Taiwan region. This low resistivity zone (LRZ) can be correlated to the common occurrence of the LRZ in the continental crust worldwide (Jones, 1987). Roecker *et al.* (1987) and Ma *et al.* (1996) also reported a low P-wave velocity zone below the highest mountain chain in Taiwan in the depth range of 20 to 30 km, about 5 km deeper than the electrical structure. The probable cause of this low resistivity zone is discussed later.

It is worth noting that the LRZ seems to migrate to the north as depth increases. This phenomenon is especially conspicuous as the depth extends to 30 to 40 km in the uppermost mantle of Taiwan (Ma *et al.*, 1996). The cause of the migration of the LRZ with depth may probably be ascribed to the tectonic activity in this area. The tectonic map of Taiwan is well documented indicating that the Wadati-Benioff zone of the Philippine Sea plate is supposed to start its subduction northward beneath the Ryukyu Island at about the latitude of  $24^{\circ}\text{N}$  (Seno, 1977). Thus, the LRZ which resides the plate begins to migrate to the north with depth.

### 3.2 Vertical NS Profiles

To examine the variations in resistivity with depth beneath Taiwan, the models were grouped into three NS profiles (Figure 7). Their locations are denoted by dashed lines in Figure 1. Line 1 is along the Western foothills, while the other two profiles are along the Central Range and the Longitudinal Valley, respectively. The value of the contours in each profile is  $\log_{10}$ (resistivity) in ohm-m units.

The resistivity structure beneath line 1 (Figure 7a) is characterized by a variable thick (10 km on average), conductive (less than  $10^{1.6}$  ohm-m) layer at the surface. On the basis of the

exposed geology, this unit corresponds to the clastic sediments (Ho, 1986). The above conductive zone is underlain by an LRZ (less than  $10^{2.2}$  ohm-m), whose bottom lies at 19-km depth to the south but deepens to 22-km to the north (Figure 7a). That is, this LRZ dips gently to the north. The dipping topography of the LRZ may probably be ascribed to the effect of the north dipping tectonic model of the Philippine Sea plate of Taiwan. As depth increases, this LRZ is underlain by a more resistive (greater than  $10^{2.4}$  ohm-m) layer.

Line 2 (Figure 7b) is along the Central Range. Therefore, this profile represents the key index to fully demonstrate the tectonic structure of Taiwan. The significant feature of the LRZ, i.e. about 20 km in thickness and dipping  $30^\circ$  northward near MT sounding 21 (latitude of  $24.5^\circ$ ) in Taiwan, is clearly displayed. These results correspond to the observations shown in the previous resistivity depth slices, providing evidence of the Philippine Sea plate subduction northward beneath Taiwan near the latitude of  $24^\circ$  N. At the northern tip of this profile, a local low resistivity anomaly (less than  $10^{1.6}$  ohm-m) extending to the depth of about 50 km is observed. This particular feature, as stated earlier, is clearly related to the Tatun geothermal area, which is the only volcanic group in Taiwan. A more resistive (greater than  $10^{2.4}$  ohm-m) layer underlies this LRZ and can be correlated to that in line 1 at great depth.

Line 3 (Figure 7c) is along the Longitudinal Valley. Generally speaking, this resistivity structure may be explained by the eastern extension of line 2. The most striking feature of line 3 is its variable thick (less than 10 km), resistive (greater than  $10^{2.4}$  ohm-m) layer at the surface. Since the metamorphic grade increases from west to east, the resistivities beneath line 3 are higher than those beneath line 2. The LRZ at about the average depth of 10 km displays a flat layer in the Longitudinal Valley and is about to subduct at MT sounding 5 at the northern end of this profile. The LRZ is underlain by a more resistive layer (ranging  $10^{2.4}$ - $10^{2.8}$  ohm-m). The P-wave tomography (Ma *et al.*, 1996) suggests that the depth of the crust of Taiwan is estimated to be 30-35 km; therefore, it can be said that the resistivities of the uppermost mantle beneath Taiwan range from  $10^{2.4}$  to  $10^{2.6}$  (250 to 630) ohm-m, which is in reasonable agreement with the experimental value of about a few hundred ohm-m worldwide (Jones, 1987).

## 4. DISCUSSION

### 4.1 Moho Discontinuity

One of the most important unanswered questions about tectonics in the Taiwan orogeny is the inference of the Moho discontinuity. From the inversion of P-wave arrival times, Yeh and Tsai (1981) suggested the crustal thickness of central Taiwan is 17 km. The inversion results from the gravity survey by Yeh and Yen (1991) assume that the oceanic crustal thickness nearby Taiwan is in the range of 10-20 km and increases from south to north. On the other hand, using the tomographic method, Ma *et al.* (1996) estimated the crust of Taiwan to be 30-35 km and that the Philippine Sea plate to be 15-20 km.

The extreme resistivity contrast between the crust and the upper mantle beneath Taiwan may have enabled those authors to detect a resistivity interface that correlates with the depth of the Moho, but this concept is quite difficult to work out when examining the resistivity patterns in Figure 7. However, from the tectonic features and the MT images, the results shown in

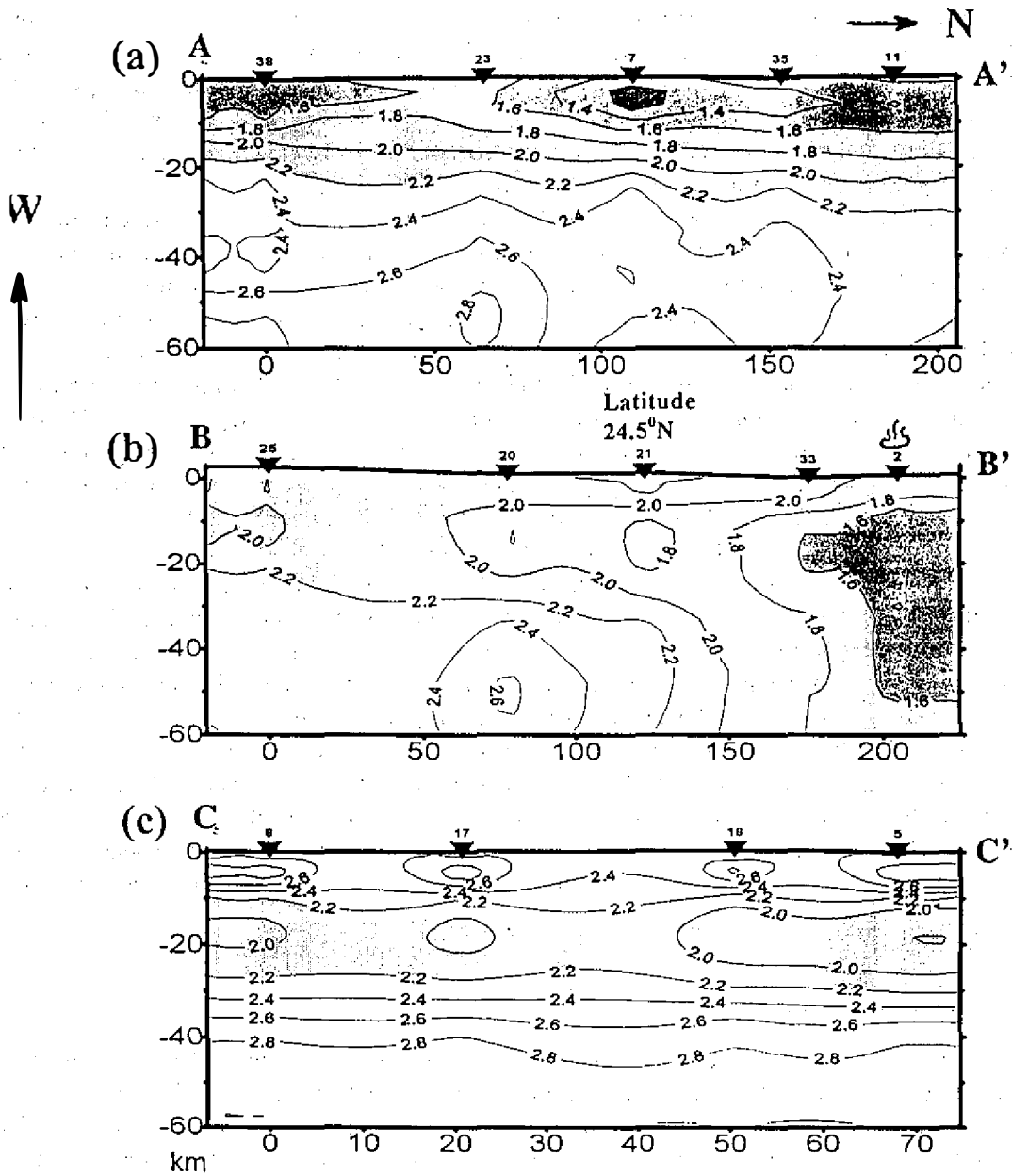


Fig. 7. NS geoelectric sections of Taiwan. (a) the Western foothills, (b) the Central Range and (c) the Longitudinal Valley. The triangles on the surface topography indicate the sounding points shown in Fig. 1. Resistivities, in  $\log_{10}$  (resistivity) ohm-m, are contoured with values lower than  $10^{22}$ =150 ohm-m shaded. The vertical scale in each plot is exaggerated for purposes of clarity. Note the north dipping conductive zone which is especially conspicuous in the Central Range.

the profiles of Figure 7 may make it easier to infer the possible electrical characteristics of the Moho region.

As Taiwan is considered to be situated where the Philippine Sea plate is subducting northward beneath the Ryukyu Islands, it indicates that the iso-resistivity contour must become deeper from south to north when it passes near 24° N. In Figure 7b, the 10<sup>22</sup> ohm-m contour is distinct and becomes deeper to the north at 24.5° N. The resistivity thus obtained is about 158 ohm-m which is consistent with the Moho estimation of resistivities of about 200 ohm-meters in neighboring Japan (Ogawa *et al.*, 1994); meanwhile its depths between 20-30 km are also close to the range of the P-wave results, 30-35 km (Ma *et al.*, 1996). However, if it is assumed that the choice of the 10<sup>22</sup> ohm-m contour is the bottom of the lowest crust, and thus regarded as the Moho discontinuity underneath Taiwan, it seems to be too shallow in light of the recent seismicity viewpoint proposing a Moho depth of about 40-50 km (Rau *et al.*, 1995; Lin, 1996).

Therefore, the resistivity boundary of the Moho beneath Taiwan is probably not as sharp as the velocity one. It is worth noting that the resistivity contour lines below the LRZ are more compressed in the Longitudinal Valley (Figure 7c) than in the Western foothills (Figure 7a). This characteristic of the resistivity pattern could reflect a regional tectonic compression history from the east of Taiwan, which then propagated and lessened to the west.

#### 4.2 LRZ

The appearance of an LRZ underneath Taiwan is both very interesting and significant. The fact that the depth to its top correlates with the depth of the top of the P-wave reflector which is believed to lie near the top of the subducting plate is remarkable. From the depth distribution of earthquakes, Wang *et al.* (1994) reported a low seismicity zone below the depth of 12 km, which is almost in the same depth range as the LRZ. Wu *et al.* (1991) also pointed out such a low seismicity zone in their seismicity profile. From theoretical studies, Barr and Dahlen (1989) and Hwang and Wang (1993) stated that a high geothermal gradient is present in the Central Range. Wang *et al.* (1994) suggested that such a geothermal effect is the most important factor contributing to the low seismicity zone. Ma *et al.* (1996) proposed that the low velocity zone underneath the Central Range and its surrounding area was probably caused by the combination of heat intrusion from the Philippine Sea plate and the effect of partial melting.

For the purpose of verifying the assumption that the low resistivity in the uppercrust of Taiwan may possibly have its origin in enhanced temperature, the transformation of resistivity to temperature was calculated and is presented below. The relationship between electrical conductivity and temperature in rocks was discussed by Keller and Frischknecht (1966). Two important mechanisms of electrical conduction exist in the rock. The first involves an intrinsic semiconduction process, in which electrons are excited into conduction bands; the second is the mechanism of conduction by ions. At high temperatures (above 500°C), the former mechanism is dominant, while in the low temperature portion, the latter mechanism is more important. Conductivity in ionic rocks resulting from the above mechanisms is usually approximated with the following equation (Keller and Frischknecht, 1966):

$$\sigma = \frac{1}{\rho} = A_1 e^{-U_1/kT} + A_2 e^{-U_2/kT}, \quad (7)$$

where T is temperature in absolute temperature; k is Boltzman's constant (  $1.38 \times 10^{-3}$  eV/°C); parameters  $A_1$  and  $A_2$  are determined by the number of ions available for conduction and their mobility through the lattice; and  $U_1$  and  $U_2$  are the activation energies required to liberate these ions. Values for the parameters of a variety of rocks are given in Table 1.

The resistivity variations were estimated at different temperatures based on Equation (7) as well as rock types in the crust; these are shown in Figure 8. Broadly speaking, the higher the temperature, the lower the resistivity observed. In addition, different rock types just shift their curves along the resistivity axis, but the curve shapes mostly remain the same (except for andesite).

If the LRZ (less than  $10^{2.2}$  ohm-m) beneath Taiwan is caused only by the enhanced temperature, the temperature should be as high as 800-1100° C based on Figure 8. However, the rise in temperature at the depth of 9 km beneath the Western foothills by only about or below 300°C is based on petroleum exploration (Suppe, 1981). This temperature rise cannot be great enough to produce such a low resistivity anomaly. The detectable low resistivity anomaly in the upper crust beneath the Western foothills in Taiwan would require the presence of other factors, the most probable of which is fluids. One possibility for the origin of fluids is through the dehydration of the crust. This has previously been suggested as an explanation for the common occurrence of low resistivities in the continental crust (Hyndman *et al.*, 1993; Jones, 1987).

It was expected by Suppe (1981) that dehydration reactions take place at a lower temperature (about 220°C) at the depth of 7 km in the Western foothills due to the drop in the fluid pressure-solid pressure ratio. The excess pore-fluid pressure may provide an indirect inference of the presence of water beneath the Western foothills (Suppe, 1981). The existence of intergranular films of water containing as little as 1% fluid can substantially lower electrical resistivity, a function of porosity (Hyndman and Shearer, 1989; Hyndman, *et al.*, 1993), and may be expected to occur at or below brittle-ductile transition (Bailey, 1990; Holness, 1993). Consequently, there are grounds to expect that a delamination surface (Koons, 1990) might be associated with a layer of anomalously low electrical resistivity.

Greenschist-zeolite facies rocks in the Central Range occur at approximately 15 km depth and may be raised and cropped out by the imbricated upthrusting of collision between the Philippine Sea plate and the Eurasian continental plate (Chen and Wang, 1995). Continuing uplift, with the topographic height of the Central Range kept approximately constant by the rapid erosion rate, maintains the enhanced temperature in the main region of uplift (Teng, 1990) and allows lateral migration of isotherms. This not only prevents rehydration through cooling but may also cause water to be released into the upper crust at increased distance from the principal region of uplift.

This implication of such dehydration reactions taking place at 10-20 km depths seems consistent with the study of depth distribution of shallow earthquakes (Wang *et al.*, 1994).

Table 1. Parameters defining the temperature dependence of resistivity in solid electrolytes (Keller and Frischknecht, 1966).

Rock	A1 (s/cm)	A2 ( s/cm)	U1 (ev)	U2 (ev)
Granite	5e-4	1e5	0.62	2.5
Gabbro	7e-3	1e5	0.70	2.2
Basalt	7e-3	1e5	0.57	2.0
Peridotite	4e-2	1e5	0.81	2.3
Andesite	6e-3	1e5	0.70	1.6

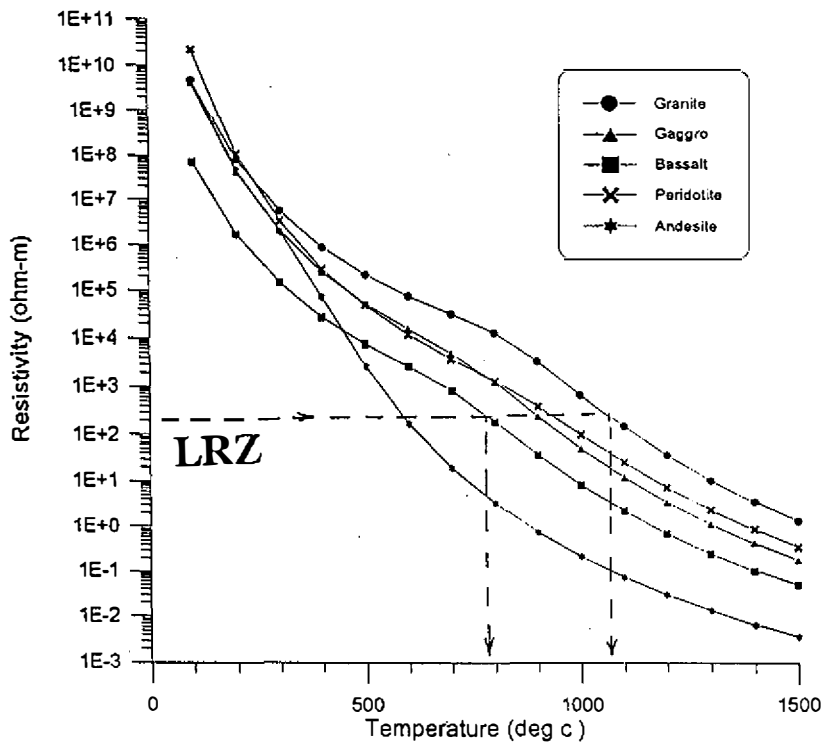


Fig. 8. Resistivity estimates based on rock types and the temperature-resistivity relationship (Keller and Frischknecht, 1966).

That study revealed that seismicity is quite low below the depth of 12 km in the Central Range. Therefore, the top of the conductive region, at about the depth of 10 km, obtained by MT soundings, corresponds with the top of the aseismic zone.

## 5. CONCLUSIONS

The MT investigation of the deep electrical structure of Taiwan has proven to be an effective tool. The existence of a distinct low resistivity zone (less than 160 ohm-m) in the uppercrust with depths ranging about 10-20 km and dipping about 30° northward near the latitude of 24.5°N beneath the Central Mountain Range is undoubtedly the most significant finding in the study. Based on the temperature estimate from the MT results, the main cause of this low resistivity zone is most probably the fluids released from dehydration reactions.

The features of the deep electrical structures are very similar to the Philippine Sea plate subduction northward beneath Taiwan. In the case of the top of the Philippine Sea plate being located at a depth only 10 km below the Central Mountain Range, it is implied that the lithosphere for Taiwan Island around the Central Range is less than 15 km in thickness. This contradicts any geologist's common sense. On the other hand, at the depth of the Moho discontinuity in Taiwan, 40-50 km, no corresponding sharp boundary can be found in the resistivity profiles. In other words, future studies are required to refine the present electrical models in order to explain and/or correct the plate tectonic model of Taiwan; however, it is suggested that several of the major deep electrical structures of Taiwan will most likely endure.

**Acknowledgments** This study was financially supported by the National Science Council of the Republic of China under grants NSC84-2111-M008-041 and NSC85-2111-M008-03. The authors thank Phoenix Geophysics for technical assistance in this pioneer MT survey in the Taiwan region. Useful comments and suggestions made by Dr. C. T. Young, Dr. F. C. Su, Mr. William Lucas and anonymous reviewers are highly appreciated.

## REFERENCES

- Aki, K., 1982: Three-dimensional seismic inhomogeneities in the lithosphere and asthenosphere. *Rev. Geophys. Space Phys.*, **20**, 161-170.
- Bailey, R. C., 1990: Trapping of aqueous fluids in the deep crust. *Geophys. Res. Lett.*, **17**, 1129-1132.
- Barr, T. D., and F. A. Dahlen, 1989: Steady-state mountain building 2: thermal structure and heat budget. *J. Geophys. Res.*, **94**, 3923-3947.
- Cagniard, L., 1953: Basic theory of the magnetotelluric method of geophysical prospecting. *Geophys.*, **18**, 605-635.
- Chen, C. H., and C. H. Wang, 1995: Explanatory notes for the metamorphic facies map of Taiwan. 2nd ed., Central Geological Survey, MOEA, Taipei, Taiwan, 51 pp. (in Chinese)
- Constable, S. C., R. L. Parker, and C. G. Constable, 1987: Occam's inversion: a practical algorithm for generating smooth models from electromagnetic sounding data. *Geo-*

- physics*, **52**, 289-300.
- Davis, J. C., 1973: Statistics and data analysis in geology. John Wiley & SONS, Inc., New York, 322-337.
- Gamble, T., W. Goubau, and J. Clarke, 1979: Magnetotellurics with a remote magnetic reference. *Geophysics*, **44**, 53-68.
- Ho, C. S., 1988: An introduction to the geology of Taiwan, explanatory text of the geological map of Taiwan. 2nd ed., Ministry of Economic Affairs, Taipei, Taiwan, 192 pp.
- Holness, M. B., 1993: Temperature and pressure dependence of quartz-aqueous fluid dihedral angles: the control of adsorbed H<sub>2</sub>O on the permeability of quartzites. *Earth Planet. Sci. Lett.*, **117**, 363-377.
- Hwang, W. T., and C. Y. Wang, 1993: Sequential thrusting model for mountain building: constraints from geology and heat flow of Taiwan. *J. Geophys. Res.*, **98**, 9963-9973.
- Hyndman, R. D., and P. M. Shearer, 1989: Water in the lower continental crust: modeling magnetotelluric and seismic reflection results. *Geophys. J. Int.*, **98**, 343-365.
- Hyndman, R. D., L. L. Vanyan, G. Marquis, and L. K. Law, 1993: The origin of electrically conductive lower crustal continental crust: saline water or graphite? *Phys. Earth Planet. Inter.*, **81**, 325-344.
- Ingham, M., 1988: The use of invariant impedances in magnetotelluric interpretation. *Geophys. J.*, **92**, 165-169.
- Jones, A. G., 1987: MT and reflection: an essential combination. *Geophys. J. R. Astr. Soc.*, **89**, 7-18.
- Keller, G. V., and Frischknecht, F. C., 1966: Electrical methods in geophysical prospecting. Pergamon Press Inc., 16-19.
- Koons, P. O., 1990: Two-sided orogen: collision and erosion from the sandbox to the Southern Alps, *New Zealand Geology*, **18**, 679-682.
- Lin, C. H., 1996: Crustal structures estimated from arrival differences of the first P-waves in Taiwan. *J. Geol. Soc. China*, **39**, 1-12.
- Ma, K. F., J. H. Wang, and D. Zhao, 1996: Three-dimensional seismic velocity structure of the crust and uppermost mantle beneath Taiwan. *J. Phys. Earth*, **44**, 85-105.
- Ogawa, Y., Y. Nishida, and M. Makino, 1994: A collision boundary imaged by magnetotellurics, Hidaka Mountain, Central Hokkaido, *Japan. JGR*, **99**, 22373-22388.
- Rau, R. J., and F. T. Wu, 1995: Tomographic imaging of lithospheric structures under Taiwan. *Earth Planet Sci. Lett.*, **133**, 517-532.
- Roecker, S. W., Y. H. Yeh, and Y. B. Tsai, 1987: Three-dimensional P and S wave velocity structures beneath Taiwan: deep structure beneath an arc-continent collision. *J. Geophys. Res.*, **92**, 10547-10570.
- Seno, T., S. Stein, and A. E. Gripp, 1993: A model for the motion of the Philippine Sea plate consistent with NUVEL-1 and geological data. *J. Geophys. Res.*, **98**, 17941-17948.
- Seno, T., 1977: The instantaneous rotation vector of the Philippine Sea plate relative to the Eurasian plate. *Tectonophysics*, **42**, 209-226.
- Stanley, W. D., J. E. Boehl, F. X. Bostick, and H. W. Sith, 1977: Geothermal significance of magnetotelluric sounding in the eastern Snake River Plain - Yellowstone region. *JGR*,

- 82, 2501-2514.
- Suppe, J., 1981: Mechanics of mountain building and metamorphism in Taiwan. *Mem. Geol. Soc. China*, **4**, 67-89.
- Swift, C. M., 1967: An MT investigation of an electrical conductivity anomaly in the SW United States. Ph.D. thesis, M. I. T., Cambridge.
- Teng, L. S., 1990: Geotectonic evolution of late Cenozoic arc-continental collision in Taiwan. *Tectonophysics*, **183**, 57-76.
- Thurber, C. H., and K. Aki, 1987: Three-dimensional seismic imaging, *Annu. Rev. Earth Planet Sci.*, **15**, 115-139.
- Tsai, Y. B., 1986: Seismotectonics of Taiwan. *Tectonophysics*, **125**, 17-37.
- Vozoff, K., 1972: The MT method in the exploration of sedimentary basins. *Geophys.*, **37**, 98-141.
- Wang, J. H., 1988: b values of shallow earthquakes in Taiwan. *Bulletin of the Seismological Society of America*, **78**, 1243-1254.
- Wang, J. H., K. C. Chen, and T. Q. Lee, 1994: Depth distribution of shallow earthquakes in Taiwan. *J. Geol. Soc. China*, **37**, 125-142.
- Ward, D. R., H. W. Smith, and F. X. Bostick, 1971: Crustal investigations by the magnetotelluric tensor impedance method. The structure of the Earth's Crust, *AGU Mono.* **14**, 397-416.
- Wu, F. T., 1978: Recent tectonics of Taiwan. *J. Phys. Earth*, **26**, 265-299.
- Wu, F. T., D. Salzberg, and R. J. Rau, 1991: The modern orogeny of Taiwan. TAICRUST Workshop Proceedings, National Taiwan Univ., Taipei, 49-62.
- Young, C. T., and M. R. Kitchen, 1989: A magnetotelluric transect in the Oregon Coast Range. *JGR*, **94**, 14,185-14,193.
- Yeh, Y. H., and Y. B. Tsai, 1981: Crustal structure of central Taiwan from inversion of P-wave arrival times. *Bull. Inst. Earth Sci., Acad. Sin.*, **1**, 83-102.
- Yeh, Y. H., and H. Y. Yen, 1991: gravity anomalies of Taiwan and their tectonic implications. TAICRUST Workshop Proceedings, Nat'l. Taiwan Univ., Taipei, 175-184.